STATIC ANALYSES OF THE EFFECT OF DEEP EXCAVATION ON THE BEHAVIOUR OF AN ADJACENT PILE IN SAND

Sameh ASHOUR [*] ![ID]

Yeşim S. ÜNSEVER [*] ![ID]

Abstract: The influence of deep excavation on adjacent pile behaviour is an important issue to ensure its serviceability and stability. In this paper, the effect of deep excavation on an adjacent loaded single pile in saturated cohesionless soil was investigated by 3D finite element method. After verification of finite element model using centrifuge test results found in literature, a parametric study was conducted by varying the most influence factors on the pile behaviour such as excavation depth, distance from the pile to the excavation and pile head type. It was concluded that the excavation depth (H_e) with respect to pile length (L_p) has a significant effect on pile response. Among the three cases of H_e/L_p, the case of $H_e/L_p = 0.5$ induced the maximum bending moment while the case of $H_e/L_p = 1.5$ induced the maximum pile lateral deflection. Moreover, the distance from the pile to the excavation site has also a significant influence on pile response and the induced bending moment in pile is inconsiderable after 9 m distance. Also, it is observed that the pile head type has an important effect on the pile behaviour especially in case of rigid head case.

Keywords: Deep excavation, single pile, finite element method, sand

Kum Zemindeki Bir Derin Kazının Komşu Kazığın Davranışı Üzerindeki Etkisinin Statik Analizi

Öz: Bitişik kazık davranışı üzerindeki derin kazı etkisinin incelenmesi, kazığın hizmet verebilirliğini ve stabilitesini değerlendirmek için önemli bir konudur. Bu çalışmada, bitişik yüklü tekil kazık üzerindeki derin kazının etkisi, doymuş kohezyonsuz zeminde, 3D sonlu elemanlar yöntemi kullanılarak araştırılmıştır. Literatürde bulunan santrifüj deney sonuçları kullanılarak sonlu elemanlar modelinin doğrulanmasından sonra; kazı derinliği, kazıkla kazı alanına olan mesafe ve kazık başı tipi gibi kazık davranışına en fazla etki eden faktörler üzerinde parametrik bir çalışma yapılmıştır. Kazık uzunluğuna göre kazı derinliğinin kazık davranışı üzerinde önemli bir etkiye sahip olduğu sonucuna varılmıştır. Üç farklı H_e/L_p durumu arasında, $H_e/L_p = 0.5$ durumu maksimum eğilme momentine neden olurken, $H_e/L_p = 1.5$ durumu maksimum kazık yanal sapmasına neden olmuştur. Ayrıca kazıktan kazıya olan mesafe de kazık tepkisi üzerinde önemli bir etkiye sahiptir ve kazıkta aktive olan eğilme momenti 9 m mesafeden sonra etkisini kaybetmiştir. Son olarak kazık başlığı tipinin kazık davranışı üzerinde önemli bir etkisi olduğu görülmüştür, özellikle rijit başlık durumunda bu etkiler daha dikkat çekicidir.

Anahtar Kelimeler: Derin kazı, tekil kazık, sonlu elemanlar yöntemi, kum zemin

1. INTRODUCTION

Due to rapid urbanization and lack of lands in urban spaces, the problem of converge buildings began to emerge. So in these areas, the construction of high-rise buildings with basements and construction of underground facilities (such as tunnels and metro stations)

[*] Bursa Uludağ University, Faculty of Engineering, Civil Eng. Dept. 16059 Bursa/Turkey
    İletişim Yazarı: Yeşim S. ÜNSEVER (unsever@uludag.edu.tr)

besides the pre-constructed buildings are common. Especially, high-rise buildings absolutely require deep excavation to reach to the formation level. One of the problems of deep excavation in urban spaces is the ground settlements of nearby buildings due to the lateral movement of the soil towards the excavation site and effective stresses release in the lateral soil. In that case, lateral soil movement will cause extra bending forces, lateral movements, and settlements on surrounding pile-supported buildings. It has been interested in this topic because of the significant effects of deep excavation on ground movements and, as a result, on nearby existing buildings, which many contractor could be faced during building new structures near existed one.

The underground infrastructures and excavating works for basement construction beside existing buildings absolutely will lead to lateral movements in surrounding soil due to stress relief. This situation requires to take into account the safety of these buildings as well as ensure the stability of the foundations that support them (Soomro et al. 2019, Liyanapathirana and Nishanthan 2016, Finno et al. 1991 and Goh et al. 2003). According to field measurement data, the braced deep excavation has a significant effect on adjacent piled foundation buildings, and the pile responses to soil movements should be taken into account during design (Zhang et al. 2018).

Poulos and Chen (1996, 1997) developed design charts to estimate the induced lateral deflection and bending moment on the single pile adjacent to unsupported and supported excavation in clayey soil, respectively, by using a two stage analysis involving the finite element method and the boundary element method. Goh et al. (2003) carried out an actual full scale test to investigate the pile behaviour near to strutted excavation in multilayer soil.   Ong et al. (2006) conducted a set of centrifuge model tests to examine the behaviour of a single pile due to unbraced excavation behind a stable wall in clay. They concluded that the decrease in pile response related highly on increasing the distance between the pile and the wall and the soil may continue to move with time after the end of excavation.

Li et al. (2014) examined the effect of deep excavation adjacent to pile by employing the Modified-Cam Clay constitutive model in explicit finite difference code FLAC3D. They studied many of influence factors such as excavation depth, pile head type, pile stiffness, distance between the pile and excavation and the axial load. The results showed that the increasing in pile response related with increasing of excavation depth. Moreover, for a fixed head pile it was noticed that a significant positive bending moment developed at pile head. Liyanapathirana and Nishanthan (2016) conducted a parametric study by using ABAQUS software to establish the pile responses due to deep excavation in clay. They found that the pile head fixity, stiffness and spacing of wall support system have a significant influence on pile response. Similar work conducted by Zhang et al. (2018), they concluded that the maximum value of lateral deflection and bending moment of pile decreases significantly with increasing distance from the excavation face. Moreover, the pile response depends upon the pile head type significantly, and the increasing of axial load has no impact on pile behaviour. Soomro et al. (2019) studied the single pile response due to adjacent excavation in saturated soft kaolin clay. They concluded that the pile behaviour strongly depends upon formation level of the excavation and embedded depth of wall.

Leung et al. (2000) studied a single pile response due to unpropped deep excavation in dense sand by conducting two centrifuge model tests in case of a stable wall and a collapse wall. They found that the pile head type has an important role on pile response. Leung et al. (2003) established the effect of unpropped excavation on pile group behaviour in sand; centrifuge model tests were carried out on pile group with free and cap head. It was found that the existence of front piles leads to decrease the induced effects in rear piles significantly. As well as, the existence of cap lead to reduce pile group response. Choudhury et al. (2006) conducted centrifuge model tests to investigate the pile responses due to excavation in sand with considering different relative densities. The test results appeared that the maximum bending

moments located near the pile mid, and increases significantly as the distance of pile from excavation decreases. Both magnitude of bending moments and pile deflection increase as excavation depth increases. Ding and Qiao (2014) conducted 2D numerical studies on pile behaviour caused by deep excavation in clayey soil overlaying rock by using the software Plaxis. A number of influence factors were investigated. As the entire pile was located in clayey soil, the largest deflection was observed at the pile toe, and when the pile went into rock soil layer, the maximum deflection was found at the pile head. Moreover, when the pile length was increased, a significant difference in the moment profile was observed. Nishanthan et al. (2016) was used Abaqus software to established the effect of shielding in pile groups close to unbraced and braced excavations utilizing different pile group designs and two head conditions (free and capped). The results showed that the deleterious impacts in unbraced excavation on the rear piles can be decreased by the existence of front piles. Furthermore, in unbraced excavation, the deflection of pile group can reduce highly. In contrast, in braced excavation these factors have less significant impact on pile group response. Ng et al. (2017) examined the influence of a multi-propped deep excavation in-flight on an adjacent pile in dry Toyoura sand; three centrifuge model tests (i.e., free, pinned and fixed-head pile) were conducted. As well as, 3D numerical analyses were carried out to verify the results of centrifuge tests. The results revealed that the restriction of pile head lead to a huge bending moment, and it may exceed bending capacity of pile. Shakeel and Ng (2017) used three dimensional coupled consolidation analysis to study 2x2 pile group response adjacent to deep excavation in soft clay. The influence of excavation depth, pile length, pile group location from excavation, stiffness of the supporting system, soil state and permeability and working load are studied.

This paper aims to investigate a loaded single pile behaviour due to propped deep excavation in saturated sandy soil by using Plaxis 3D finite element program. After validation the finite element solution, the parametric studies are conducted to describe the pile response due to adjacent excavation. The pile response will include the bending moment, lateral deflection and settlement of the pile. For this purpose, 3D finite element model will be developed, which takes account of small-strain stiffness. The validated model will be utilized to study the most influencing factors on the pile behavior (i.e., excavation depth, distance from the pile to excavation, pile head type).

2. VALIDATION OF NUMERICAL FINITE ELEMENT MODEL USING CENTRIFUGE TEST RESULTS

2.1. Description of the Centrifuge Test

The 3D finite element model that will be used in this parametric study has been validated using centrifuge test conducted by Ong et al. (2006). The centrifuge test was carried out at the National University of Singapore at a centrifuge acceleration of 50g to investigate the pile behaviour due to adjacent excavation in soft clay in case of stable retaining wall. The model container made from stainless steel with internal dimensions 540 mm long, 200 mm wide and 470 mm high. The container firstly filled by Toyoura sand by raining method with a thickness of 120 mm (6 m in prototype scale) then the Malaysian kaolin clay, mixed with water and became a slurry, was filled up to a depth of 130 mm (6.5 m in prototype scale) above the sand layer. The clay was gradually consolidated until a maximum surcharge pressure of 20 kPa. A filter paper was placed between the sand and clay to prevent mixing of them during experiment. Water tightness of the container was supplied by rubber seals. The pile model used in the centrifuge test was from a hollow square aluminum tube and instrumented with 10 pairs of strain gauge, the total length of the pile is 350 mm with a soil embedment depth of 250 mm and the wall model was a 3 mm-thick alumium plate. Those models were installed into the soil by jacking them. The method of draining ZnCl2 is employed to simulate the soil excavation. During the test the excavation was carried out by draining ZnCl2 solution at 50g in six stages

over two days. More details about the centrifuge test can be found in Ong et al. (2006). Figure 1 shows the cross section and plane view of the centrifuge model conducted by Ong et al. (2006) in prototype scale.
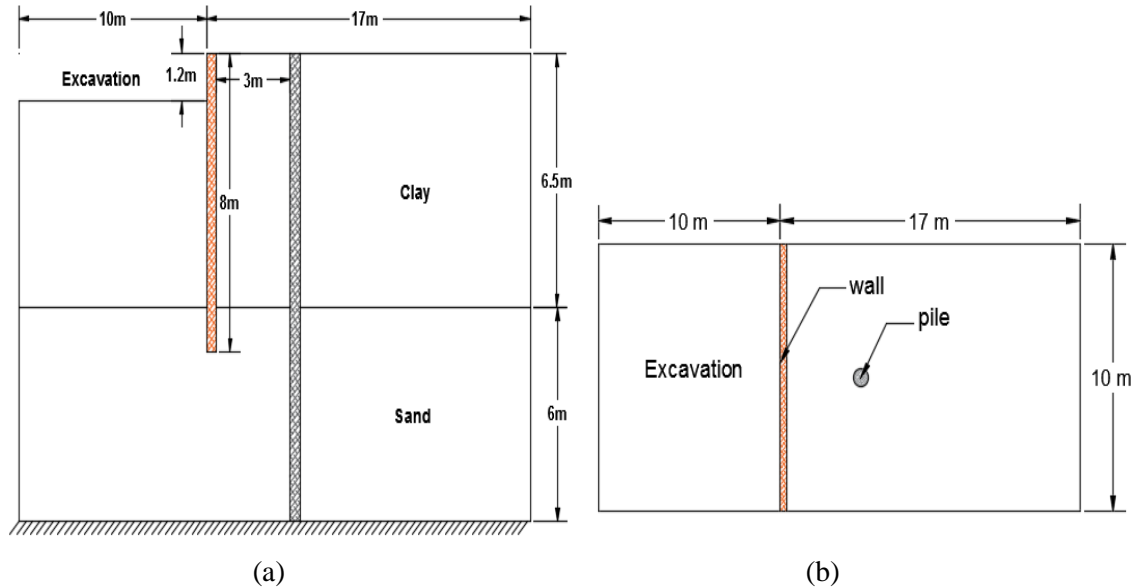

(a) (b)

Figure 1:
***a.** Cross section **b.** Plane view of the centrifuge model conducted by Ong et al. (2006) in prototype scale*

2.2. Materials Properties Used in the Centrifuge Test

The simulation of the centrifuge test was carried out by using Plaxis 3D finite element program. The kaolin clay used in centrifuge test was simulated with Modifiy Cam Clay (MCC) model which is suitable to simulate the behaviour of normally consolidated soft soils (Plaxis 3D Material Models V20). Table 1 summarized the kaolin clay properties used in the finite element analysis (Ong et al., 2006, Teh et al., 2005). The Toyoura sand, used in centrifuge test was simulated using Hardening soil model (HS) which is suitable to simulate the behaviour of sandy soil (Plaxis 3D Material Models V20). Table 2 summarized the Toyoura sand properties used in the finite element analysis (Leung et al., 2000).

The pile model used in the centrifuge test was from a hollow square aliminium tube with a prototype bending rigidity, EI of 2.2×10^5 kN. m^2, which is equivalent to a 600 mm diameter cast in situ Grade 35 concrete bored pile with length of 12.5 m in protoype scale. Table 3 summarized the pile properties used in the finite element analyses. The retaining wall model was a 3 mm-thick aliminium plate with a prototype bending moment of 24×10^3 kN. m^2/m, which is equivalent to a FSP-IIA sheet pile with total depth of 8 m in prototype scale. The elasticity modulus of steel is 210 MPa.

Table 1. MCC soil parameters for Kaolin clay

Parameter	Value	Reference
Unit weight, γ (kN/m^3)	15.21	Ong et al. (2006)
Cam-clay compression index (λ)	0.244	Deduced from compression and swelling index
Cam-clay swelling index (κ)	0.053	
Tangent of the critical state line (M)	0.9	Teh et al. (2005)
Coefficient of permeability (m/s)	1.36×10^{-8}	Ong et al. (2006)

Effective friction angle, $\phi'(°)$	23	Ong et al. (2006)
K_0 value for normal consolidation, K_0^{nc}	0.6	Ong et al. (2006)
Poisson's ratio, (v)	0.3	

Table 2. HS soil parameters for Toyoura sand

Parameter	Value	Reference
Unit weight, γ (kN/m^3)	15.78	Leung et al. (2000)
Triaxial compression stiffness, E_{50}^{ref} (kN/m^2)	30×10^3	Yamashita et al. (2000)
Primary oedometer stiffness, E_{oed}^{ref} (kN/m^2)	24×10^3	Deduced from measured E_{50}^{ref}
Unloading/reloading stiffness, E_{ur}^{ref} (kN/m^2)	99×10^3	Deduced from measured E_{50}^{ref}
Effective friction angle, $\phi'(°)$	43	Ong et al. (2006) and Leung et al. (2000)
Dilatancy angle, ψ (°)	15	Bolton and Powrie (1986)
K_0 value for normal consolidation, K_0^{nc}	0.318	Deduced from ϕ' value
Poisson's ratio, (v)	0.3	
Reference stress for stiffness, p^{ref} (kN/m^2)	100	

Table 3. Pile properties

| Parameter	Value
Bending rigidity (EI)	2.2×10^5 kN. m^2
Diameter	0.6 m
Length	12.5 m

2.3. Finite Element Modelling of the Centrifuge Test

As mentioned in the previous section, PLAXIS 3D finite element program was used to model the centrifuge test in prototype scale, Figure 1. Due to symmetry of loading and geometry, only one half of the problem was modelled. The size of the mesh was taken as (27 m × 10 m × 12.5 m) in X-axis, Y-axis and Z-axis, respectively. The vertical sides of the model were restrained against to the horizontal movement, while the bottom side was restrained in all directions. The top side was free to move in any direction. The pile was modelled as an embedded beam consists of beam elements which is 3-node line element, the interaction between the pile foot and pile skin and the surrounding soil was described as special interface element. A 12-node interface element was used to to describe the actual interaction between the soil and the wall. Medium type mesh was adopt in the anaylsis. The default setting of mesh refinements was used to refine the soil around the elements. The mesh consisted from 7017 soil elements and 12770 nodes.

2.4. Comparision between the Measured and Computed Results

Figure 2 shows the measured and computed lateral deflection profile along the pile and the induced bending moment due to the adjacent excavation. It was noticed that the maximum deflection occurs at the pile head in both measurements and in the analysis results. The

maximum deflection in measured results was 15 mm (1.5% from pile diameter) while the maximum deflection in computed results was 12 mm (1.2% from pile diameter), this difference decreases gradually with the depth. On the other hand, due to free head of pile, the induced bending moment for both computed and measured results was zero. According to the computed results from numerical modelling; it was noticed that the bending moment increases gradually up to maximum value of 87 kN.m at a depth of 6.5 m (52% from pile length), after 6.5 m it decreases gradually until reaching to the pile tip and becomes zero. The same trend was noticed for bending moment in measured results of centrifuge test. Generally, the computed bending moment shows a good agreement with the measured bending moments. Hence it can be adopted in the finite element analysis later in this study.
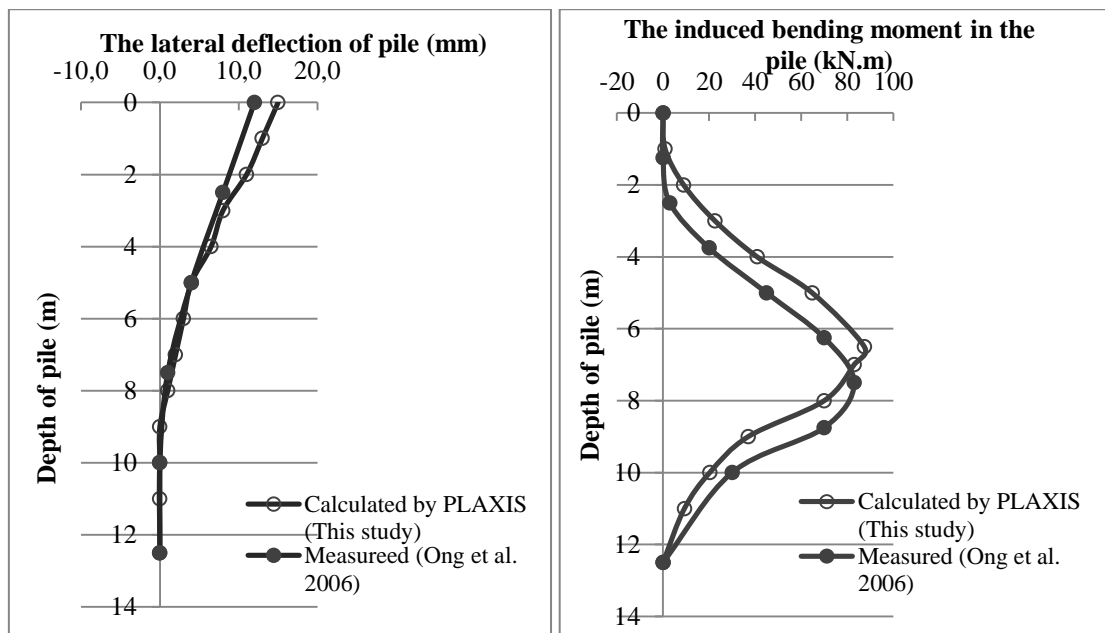
(a)   (b)

Figure 2:
*Comparision of computed and measured results **a.** pile deflection **b.** bending moment*

3. THE BEARING CAPACITY OF PILE

The pile load test was carried out using PLAXIS 3D finite element program to compute the pile bearing capacity. A single bored concrete pile with diameter of 1 m, pile length of 20 m and elastic modulus of 30 GPa was loaded gradually with a point load (with increment of 500 kN). The size of the mesh was taken as (40 m×40 m×40 m) in X-axis, Y-axis and Z-axis, respectively. The sandy soil was modelled using Hardening soil model (HS), where the sand properties are given in Table 4. The pile was modelled as an embedded beam with 3-node line element. Figure 3 shows the load-settlement curve. The settlement-based failure criterion for large diameter piles proposed by Ng et al. (2001) was used to determine the ultimate capacity of the pile. The failure criterion is given in the following equation:

$$\Delta_{ph,max} \cong 0.045 d_p + \frac{1}{2}\frac{P_h L_p}{A_p E_p} \tag{1}$$

where $\Delta_{ph,max}$ is the maximum pile head settlement corresponding to pile ultimate capacity, d_p is the pile diameter, P_h is the applied load on pile, L_p is the pile length, A_p is the pile area and

E_p is the elastic modulus of the pile. Based on the failure criterion, the ultimate bearing capacity was about 5000 kN, by taking a factor of safety of 3 the working load is determined as 1600 kN.
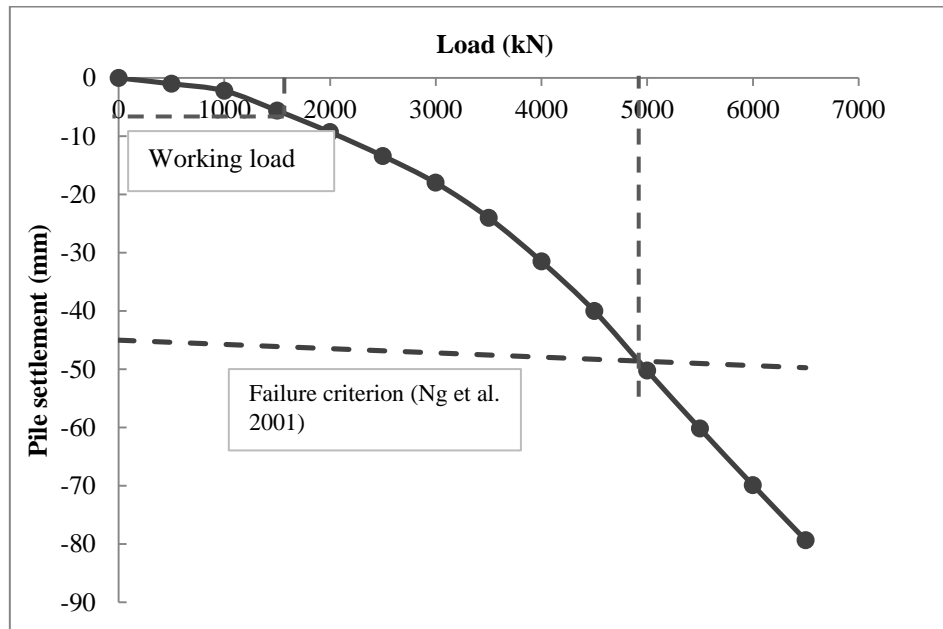
Figure 3:
Load-settlement curve computed by Plaxis 3D program

4. THREE-DIMENSIONAL FINITE ELEMENT MODEL

4.1. Properties of Finite Element Model and Boundary Conditions

Figure 4 shows the models that used in the anaylses with different cases of H_e/L_p. The ratio of H_e/L_p= 0.5, 1 and 1.5 represent the excavation above the pile toe level, at the pile toe level and below the pile toe level, respectively. The ratio of wall penetration depth to the excavation depth was 0.5 in each case (Hsiung, 2009). The excavation depth was equal to 10 m, 20 m and 30 m in the case of H_e/L_p= 0.5, 1 and 1.5, respectively. The pile length was kept as a constant, equal to 20 m. The model which has the ratio of H_e/L_p= 1 represents the typical model, shown in Figures 5 and 6. The size of the mesh was taken as (50 m × 20 m × 70 m).

In this study, the sand properties were adopted from the study of Ünsever (2015). The sand was simulated using Hardening soil model (HS). Table 4 shows the sand properties used in the analyses. The ground water table was assumed at the ground surface. The struts were spaced 2.5 m vertically and 10 m horizontally. Tables 5 and 6 show the diaphragm wall and strut properties used in the analyses, respectively. In the model, a single bored concrete pile with diameter of 1 m and length of 20 m was located at 3 m distance (center to center) from the diaphragm wall. The working load of 1600 kN was applied on the pile head. Table 7 shows the pile properties used in the analyses. The pile was modelled as an embedded beam. Maximum skin and base resistance T_{max} is the maximum traction allowed at the skin of the embedded beam which is considered to be constant along the pile. And F_{max} is the maximum compression force allowed at the foot of the embedded beam. The values selected for the bearing capacity parameters are selected based on the study of Smulders et al. (2019).
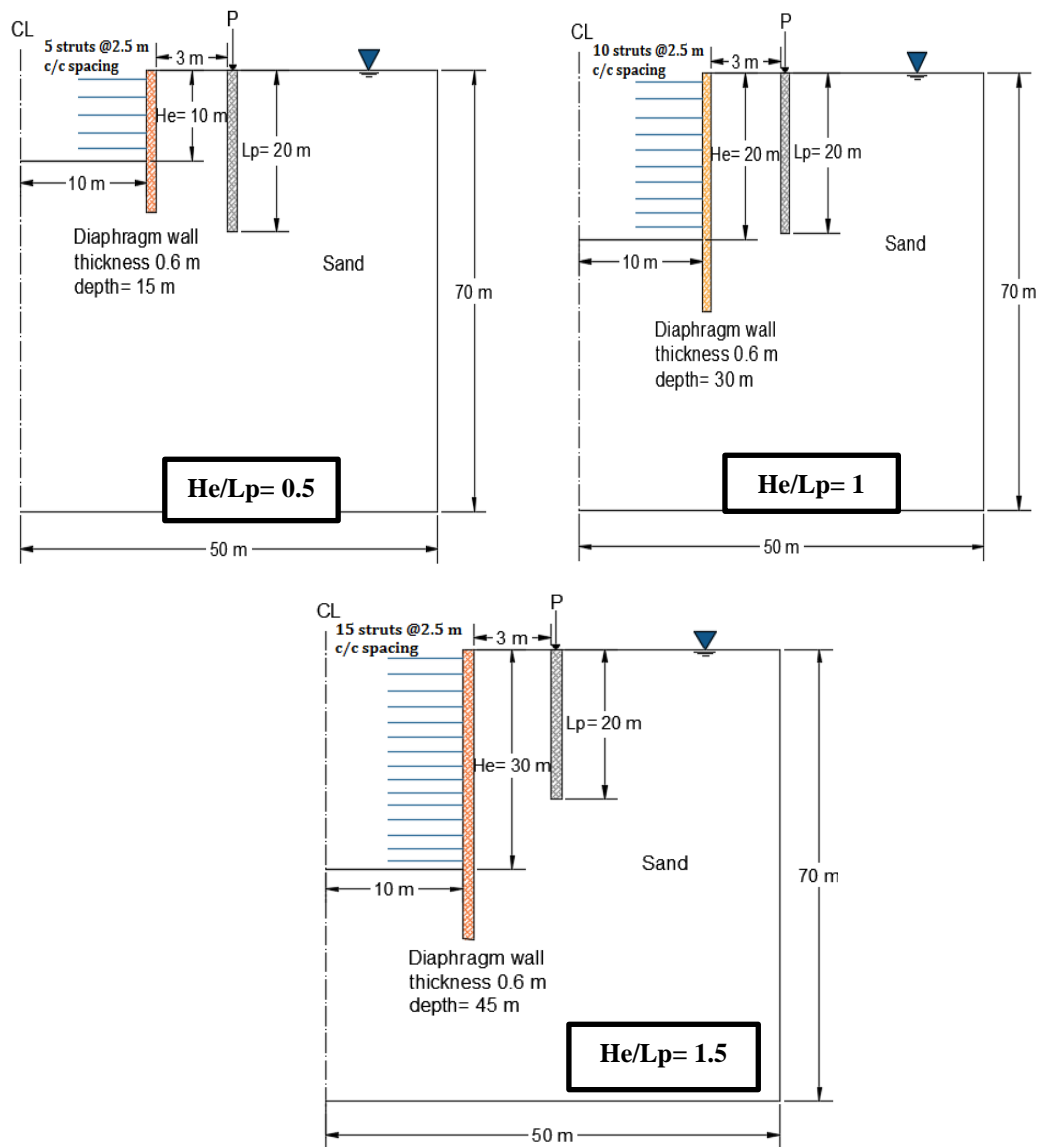
Figure 4:
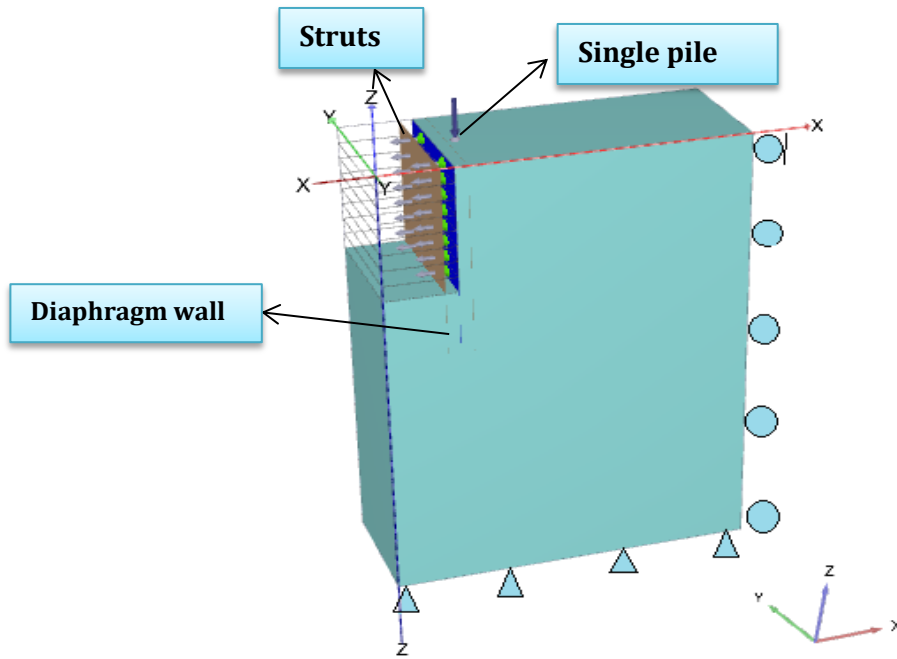*Cross section of model for three cases of H_e/L_p*
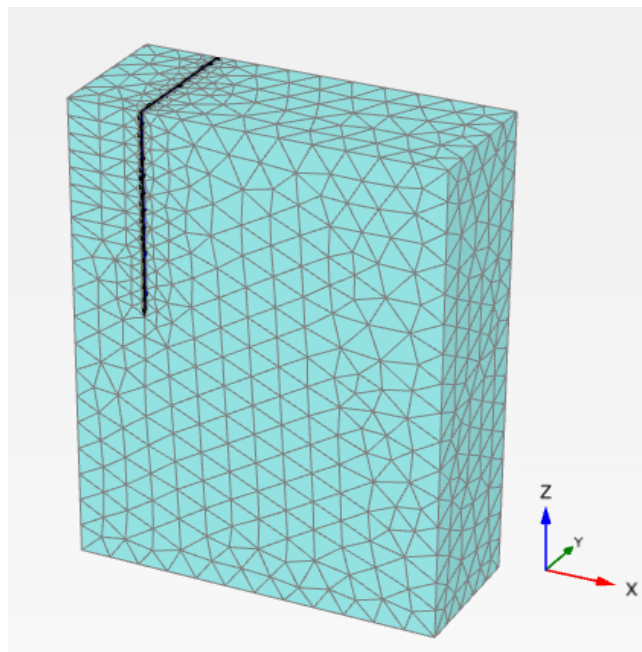
Figure 5:
Typical used finite element model

Figure 6:
Finite element mesh

Table 4. Sand properties (Ünsever, 2015)

Parameter	Value
Dry unit weight, γ_d (kN/m^3)	14.52
Saturated unit weight, γ_{sat} (kN/m^3)	19.00
Relative density, D_r (%)	70
Initial void ratio, $e_{initial}$	0.83
Triaxial compression stiffness, E_{50}^{ref} (kN/m^2)	29.56×10^3
Primary oedometer stiffness, E_{oed}^{ref} (kN/m^2)	24.65×10^3
Unloading/reloading stiffness, E_{ur}^{ref} (kN/m^2)	99.59×10^3
Effective friction angle, ϕ' (°)	43.0
Dilatancy angle, ψ (°)	15.8
K$_0$ value for normal consolidation, K_0^{nc}	0.318
Poisson's ratio, (ν)	0.19
Reference stress for stiffness, p^{ref} (kN/m^2)	100
Cohesion (kN/m^2)	0.1
Interface reduction factor	0.75

Table 5. Diaphragm wall (plate element) parameters

Parameter	Value
Unit weight , γ (kN/m^3)	25.00
Thickness (m)	0.6
Young's Modulus, E (GPa)	30.00
Poisson's ratio, (ν)	0.3

Table 6. Strut (fixed end anchor) parameters

Type	Axial rigidity	Area (m^2) ×10^{-4}	Young's Modulus (GPa)
H 150×75×5×7 steel	374.85×10^3	17.85	210.00

Table 7. Embedded pile parameters

Parameter	Value
Unit weight , γ (kN/m^3)	25.00
Young's Modulus, E (GPa)	30.00
Pile diameter, d_p (m)	1.0
Pile length, L_p (m)	20.0
Skin resistance	Layer dependent
Maximum skin resistance, T_{max} (kPa)	380
Maximum base resistance, F_{max} (kPa)	1598

5. PARAMETRIC STUDY

5.1. Effect of Excavation Depth

In order to investigate the effect of excavation depth on the pile behaviour located at 3 m behind the wall; three different cases of excavation depth to a constant pile length (H_e/L_p) were studied. As mentioned in the previous section, the ratio of H_e/L_p= 0.5, 1 and 1.5 represent the

excavation above the pile toe, at the level of pile toe and below the pile toe, respectively. The pile length was kept as a constant (equal to 20 m) during these analyses.

5.1.1. The Pile Settlement Due to The Excavation

Figure 7 shows the settlement of the loaded pile along the pile length due to the excavation in three cases of H_e/L_p. The results show that the pile settlement increases with increase of excavation depth. Moreover, the settlement is constant along the pile axis. The maximum pile settlement is 10, 20 and 37 mm (i.e., 1, 2 and 3.7% from pile diameter d_p) for the case of H_e/L_p = 0.5, 1 and 1.5, respectively. By the comparing these values with the settlement of the pile at the working load (6 mm "0.6%d_p"), it can be noticed that for all the three cases the pile settlement exceeds the allowable limit of pile settlement (Ng et al., 2001) according to the failure criterion is given in Eq. 1.
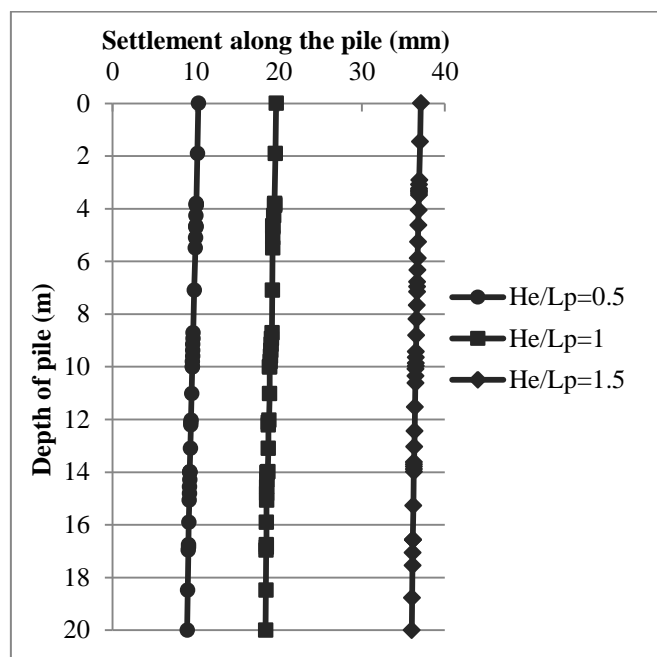

Figure 7:
The settlement of the loaded pile along the pile length due to the excavation in three cases of H_e/L_p

5.1.2. The Pile Lateral Deflection Due to The Excavation

Figure 8 shows the pile lateral deflection profile due to the excavation at the end of excavation in three cases of H_e/L_p. The vertical axis of figure was normalized as a ratio of pile length for comparison reasons. The negative values mean that the pile moves towards excavation. It can be seen from the figure that the pile deflected towards the excavation side in three cases of H_e/L_p as expected, because the excavation leads to stress release and soil displacement towards excavation. In the case of H_e/L_p= 0.5 which means the pile toe located below the final excavation level; the maximum deflection occurs at the pile head and the upper part of the pile (until 11 m of pile length) deflects towards excavation side while the lower part stays almost stable. This is because of the embedded part of the pile with respect to the excavation final level, which provides the pile stabilization. In the second case ($H_e/L_p = 1$) which means the pile toe located at the same final excavation level; both the pile head and toe

move towards the excavation side. The deflection increases from the pile head until 11 m (55% from pile length L_p) with a maximum value of 13 mm (1.3% d_p) along the pile length then it begins to decrease. In the third case ($H_e/L_p = 1.5$), which means the pile toe located above the final excavation level; it appears that both the pile head and the toe move towards the excavation side. But the pile toe deflection (equal to 24 mm) is larger than the pile head deflection. This is because of the relatively larger final excavation depth. Hence, it can be concluded that the case of $H_e/L_p = 1.5$ induces the highest lateral deflection, which occurs at the pile tip, while the case of $H_e/L_p = 0.5$ induces the lowest lateral deflection at the pile. Moreover, pile head displacements are similar for all three cases, although pile tip lateral displacements depend on excavation depth.

For comparison reason, results from centrifuge test (excavation depth was 4.5 m with no struts and the pile length was 12.5 m) conducted by Leung et al. (2000) are included in Figure 8. From the figure, it can be seen that the pile lateral deflection profile in that study shows similar behavior to the lateral deflection profile in case of $H_e/L_p = 0.5$ since they have similar conditions.
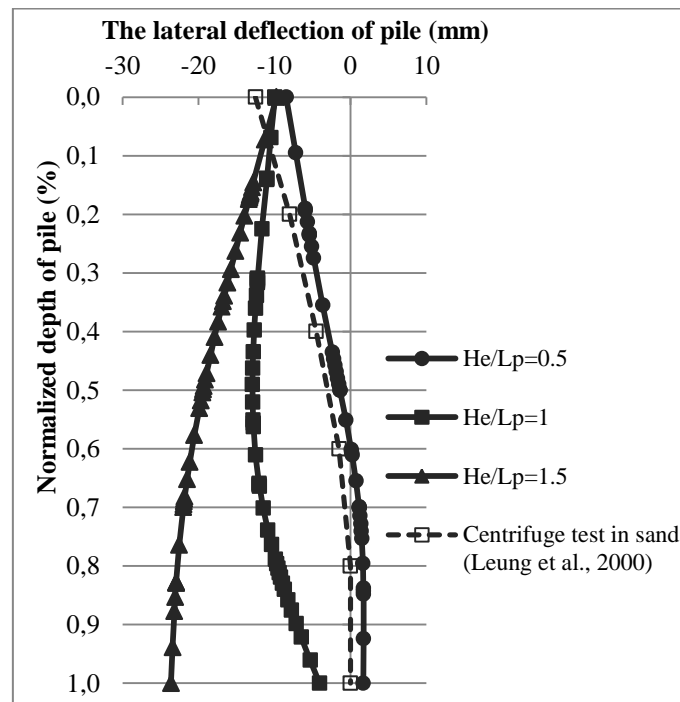

Figure 8:
The pile lateral deflection profile due to the excavation in three cases of H_e/L_p

5.1.3. The Induced Pile Bending Moment Due to The Excavation

Figure 9 shows the induced bending moment profile at the pile due to the excavation in the three cases of H_e/L_p. The negative values mean that the pile is subjected to tensile stress along the pile shaft which towards the excavation. The induced bending moment at the pile head is zero because of the free head of pile for all cases. From the figure, it can be seen that for all cases negative bending moment increases gradually at the upper part of the pile. Then, for $H_e/L_p = 0.5$ case, the moment becomes positive in the below part which increases gradually, and at the pile toe bending moment becomes zero. For the case of $H_e/L_p = 1$ and 1.5, it can seen that they show similar bending moment behavior where the negative bending moment was

induced along the whole pile shaft which means the pile shaft is subjected to a tensile stress, and at the pile toe bending moment becomes zero. Moreover, maximum bending moment occurs (positive or negative depending on the excavation depth) at about 0.7-0.75% normalized depth of the pile for all three cases. The case of $H_e/L_p = 1$ developed the highest moment because the pile toe was at the same level with the final excavation depth, while the case of $H_e/L_p = 0.5$ developed more bending moment with respect to the case of $H_e/L_p = 1.5$, since the lower part of the pile below the final excavation depth in the case of $H_e/L_p = 0.5$ was experienced higher restraint from the surrounding soil. Hence, it can be concluded that the case of $H_e/L_p = 1$ induces the highest bending moment in the pile while the case of $H_e/L_p = 1.5$ induces the lowest bending moment

For comparison reason, results from the modelling of centrifuge test (excavation depth was 8 m with 2 level of soft struts and the pile length was 20 m) conducted by Ng et al. (2017) are included in Figure 9. From the figure it can be seen that the negative bending moments induced at the ground surface and at the upper part of the pile (until $0.43L_p$) and the positive bending moment induced in the lower part. Also, it can be noticed that the pile has the same trend of bending moment profile in case of $H_e/L_p = 0.5$ that analyzed in this study but the values were relatively larger especially at the upper part of the pile. Another results from centrifuge test conducted by Leung et al. (2000) are included in the same figure. From the figure it can be seen that only positive moment induced along the pile length with maximum value occurs at about 0.6% of the normalized depth of the pile. Thus it can be said that the different conditions of each analysis and test actually lead to different results in induced bending moment profile of a pile depending on the pile slenderness, pile head connection, excavation depth, etc.
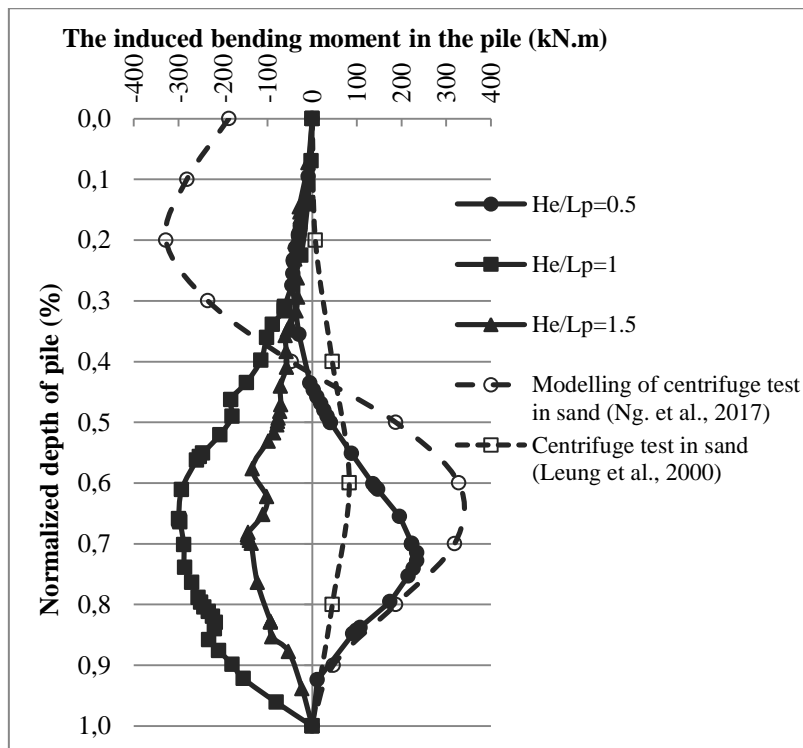

Figure 9:
The induced bending moment profile in the pile due to the excavation in three cases of H_e/L_p

5.2. Effect of the Distance From the Pile to Excavation on the Pile Response

In order to investigate the effect of horizontal distance on the pile behaviour due to the excavation; six distances 3, 5, 7, 9, 11 and 20 m (i.e., 15%, 25%, 35%, 45% and 55% and 100% from the final excavation depth H_e) were studied. The final excavation depth and pile length were kept constant, equal to 20 m ($H_e/L_p= 1$). Figure 10(a) shows the pile lateral deflection distribution due to changing distances between the pile and the excavation site at the end of excavation. It can be seen that the increasing of distance from the pile to the excavation (X) leads to decrease the lateral deflection of pile as expected, where the deflection profile totally changes from curve to a line as the distance increases. Also, it can be noticed that the pile head deflection is same for the first five cases but decreases significantly when the distance equal to 20 m. Moreover, the pile toe deflection decreases as the distance increases.

Figure 10(b) shows the profile of induced bending moment at the pile due to changing the distance from pile to the excavation site. It can be seen that the increasing of distance from pile to the excavation site leads to decreasing the bending moment in the pile significantly. In the first three cases (3, 5 and 7 m), a negative bending moment was induced along the pile shaft. After 11 m distance, only positive bending moment induces in the pile with insignificant values. It can be said that, the induced bending moments on the pile are negligible after 9 m distance between the pile and the excavation.
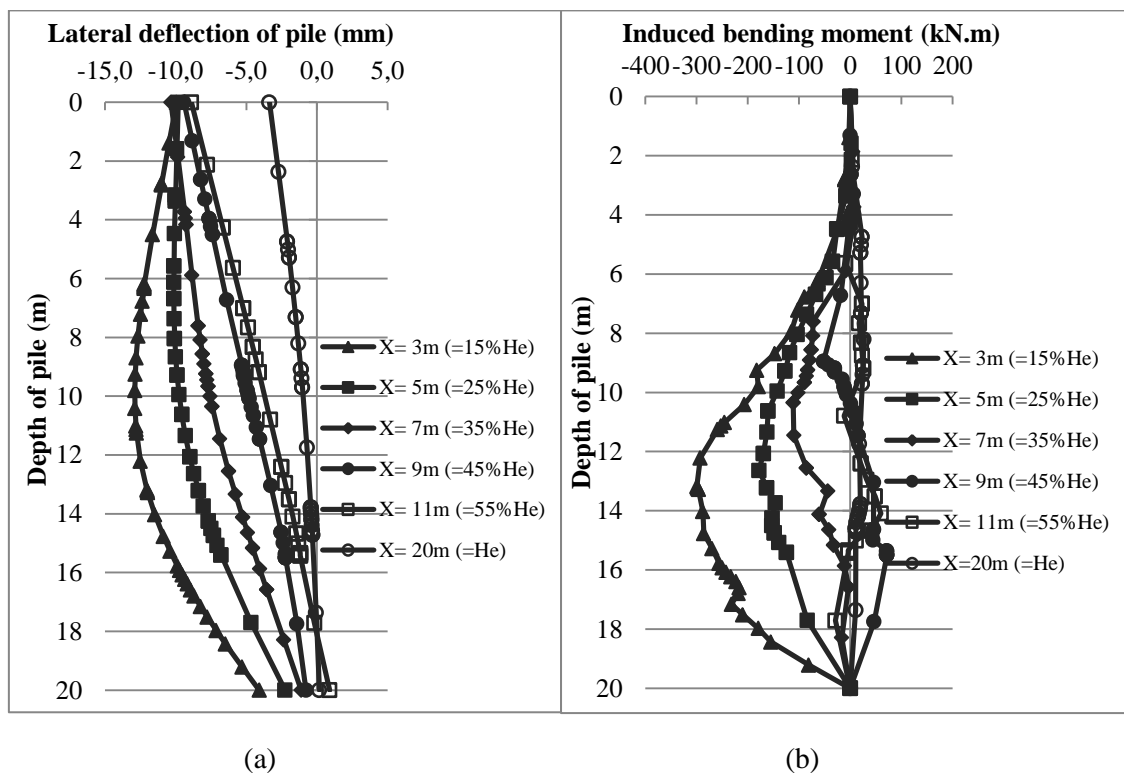

(a)   (b)

Figure 10:
The effect of distance from the pile to excavation on pile response (a) Pile deflection (b) Bending moment

5.3. Effect of the Pile Head Type

Figures 11(a), (b) and (c) show the lateral deflection of pile due to adjacent excavation in case of free, hinged and rigid pile head for the case of $H_e/L_p= 0.5$, 1 and 1.5, respectively. The

hinged head represents the case of pile group which connected with a beam, while the rigid head represents the case of piles restrained by a rigid raft. It can be seen from the figure that the deflection at the pile head was zero in the case of rigid head of pile in the three cases as expected, this is because of the pile head is restrained from any movement in horizontal and vertical directions. Generally, in the case of hinged and rigid head, the pile deflection is smaller in the upper part of the pile (about $0.5L_p$) than that of the free head case. Also it can be seen that the maximum deflection was about at the mid of the pile in the case of $H_e/L_p= 1$, while the maximum deflection was at the pile toe in the case of $H_e/L_p= 1.5$ for all head pile conditions. In addition, as it is seen from the figures, the pile head connection effects the lateral displacements at the upper part of the pile, where the behavior difference is more significant in the case of $H_e/L_p= 0.5$. At the lower part of the pile all head connections show similar behavior and deformation amount as expected.

For comparison reason, results from centrifuge test (excavation depth was 8 m with 2 level of soft struts and the pile length was 20 m) conducted by Ng et al. (2017) are included in Figure 11(a) which is similar to the case of $H_e/L_p= 0.5$. Another results from centrifuge test (excavation depth was 4.5 m with no struts and the pile length was 12.5 m) conducted by Leung et al. (2000) are also included in the same figure. From the figure, it can be noticed that the pile moves totally towards the excavation and the deflection profile is similar for both centrifuge tests. But the lateral deflection in the case of $H_e/L_p= 0.5$ differs slightly from these centrifuge test results, this is may be attributed to the soft struts and wall properties that used in the tests.

Figures 12(a), (b) and (c) show the induced bending moment of pile in case of free, hinged and rigid pile head for case of $H_e/L_p= 0.5$, 1 and 1.5, respectively. The negative values mean that the pile is subjected to tensile stress along the pile shaft. Due to restriction of the pile head movement in case of rigid head, higher positive bending moment was induced at the pile head. It was noticed that as the excavation depth increases the induced positive bending moment at the pile head increases. Among the three cases the positive bending moment was 1927 kN.m (i.e., 154% from bending capacity of pile) in the case of $H_e/L_p= 1.5$ and 1507 kN.m (i.e., 120% from bending capacity of pile) in the case of $H_e/L_p= 1$, respectively, both overcomes the bending capacity of pile 1250 kN.m corresponding to 1% steel (ACI Committee 318, 2005). Hence it can be concluded that the pile head type and excavation depth effect significantly on the pile response during the adjacent excavation especially in the case of rigid pile head where high positive bending moment induces at the pile head, which can exceed the bending capacity of pile.

For comparison reason, results from two centrifuge tests that mentioned above were included in the Figure 12(a). From the figure it can be obviously seen that the the tests results have the same trend of induced bending moment in case of rigid and hinged head. However, the results obtained by Ng et al. (2017) were higher, this can be attributed to support system stiffness that used in the tests. Thus it can be said that the different conditions of each analysis and test actually lead to different results in induced bending moment profile.

If Figure 11 and 12 are evaluated together, the pile head connection importance can be understood better. Although rigid head connection seems to have advantage according to lateral deflection results, since it has smallest displacements in all three cases, the evaluation of bending moment graphs show largest bending moments on the pile head regardless of excavation depth for the rigid head connection case. On the other hand, free and hinged connections show similar bending moment behaviours, which are pretty smaller than rigid head connection. For free head connection case, larger lateral deflections are observed comparing to hinged and rigid head connection results. For that reason, it is seen that hinged connection gives better performance according to considering lateral deflection and bending moment results.

6. SUMMARY AND CONCLUSIONS

This paper studied the behaviour of a single pile due to adjacent deep excavation in saturated cohesionless soil by using 3D finite element method. After verification of finite element model using centrifuge test results found in literature; a parametric study was conducted to investigate the influence of some factors on pile behaviour such as excavation depth, distance from pile to the excavation site and pile head type. Working load is applied on the pile head and pile length is constant through the study.

The following conclusions are drawn according to the finite element analyses results: The maximum pile settlements (1, 2 and 3.7% from pile diameter d_p for the case of $H_e/L_p = 0.5$, 1 and 1.5, respectively) due to the excavation exceed working load settlement which is %0.6 of the pile diameter. The case of $H_e/L_p = 1.5$ induces the maximum lateral deflection, which is 24 mm, occurs at the pile tip, while the case of $H_e/L_p = 0.5$ induces the lowest lateral deflection which is calculated as 10 mm, occurs at the pile head. Among the three cases of H_e/L_p, where the case of $H_e/L_p = 1$ induces the maximum bending moment in the pile, which is 299.44 kN.m while the case of $H_e/L_p = 1.5$ induces the minimum bending moment which is 143.66 kN.m. When the distance from pile to the excavation site is considered, the pile lateral deflection decreases significantly with the increase of the distance between the pile and excavation site, while after 9 m distance the bending moments in the pile are negligible.

In case of rigid head pile connection, a significant positive moment was induced at the pile head which is 1927 kN.m and 1507 kN.m (i.e., 154% and 120% from bending capacity of pile) depending on the excavation depth of $H_e/L_p = 1$ and 1.5, respectively. Maximum lateral deflection is calculated as 23 mm at the pile tip for the case of $H_e/L_p = 1.5$ regardless of head connection. However, for smaller excavation depths, free head connection shows larger lateral deflections than rigid and hinged connections.

Thus it can be said that the depending on the distance and depth of the excavation and also depending on the soil and pile properties, a new excavation site may effect the stability of the existing pile structure severly if the necessary precautions are not taken.
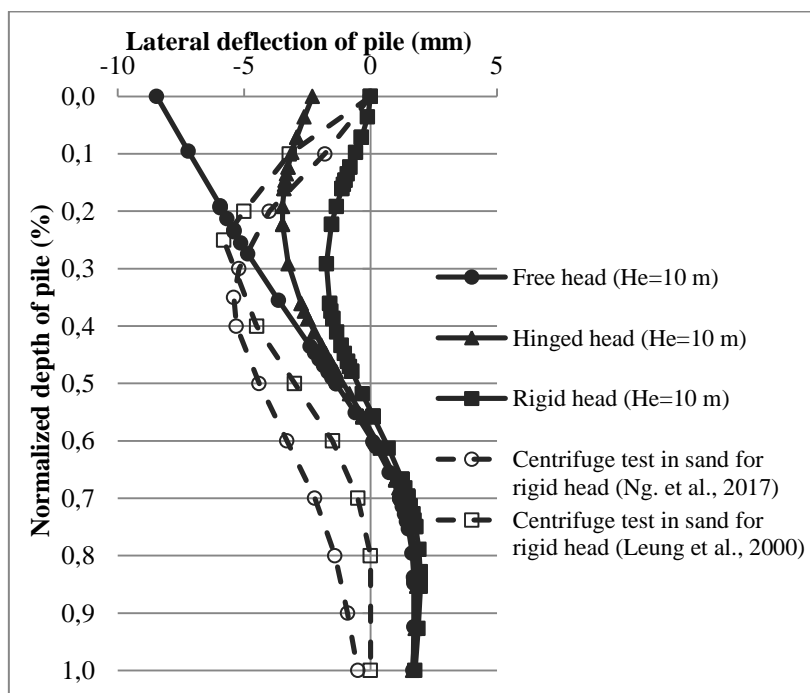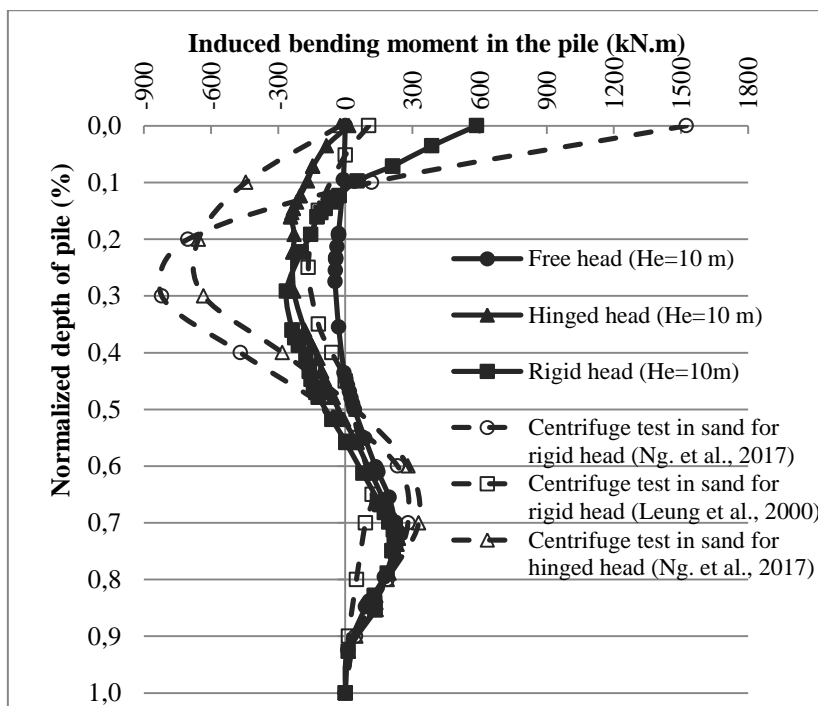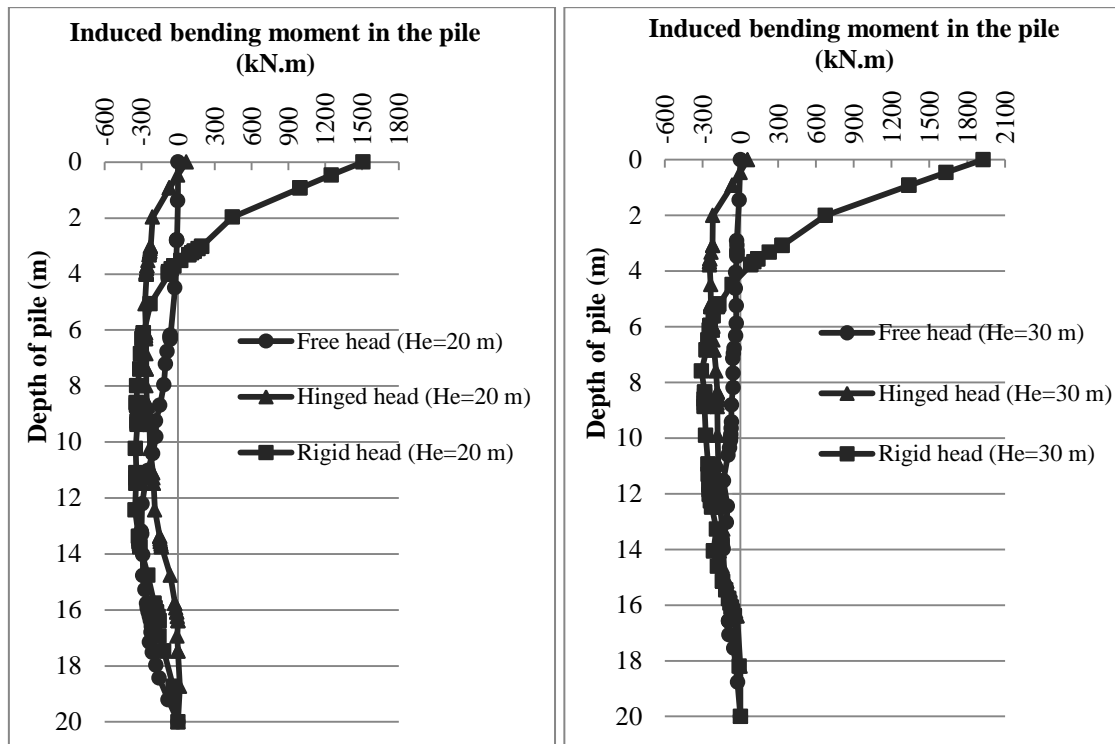
(a)
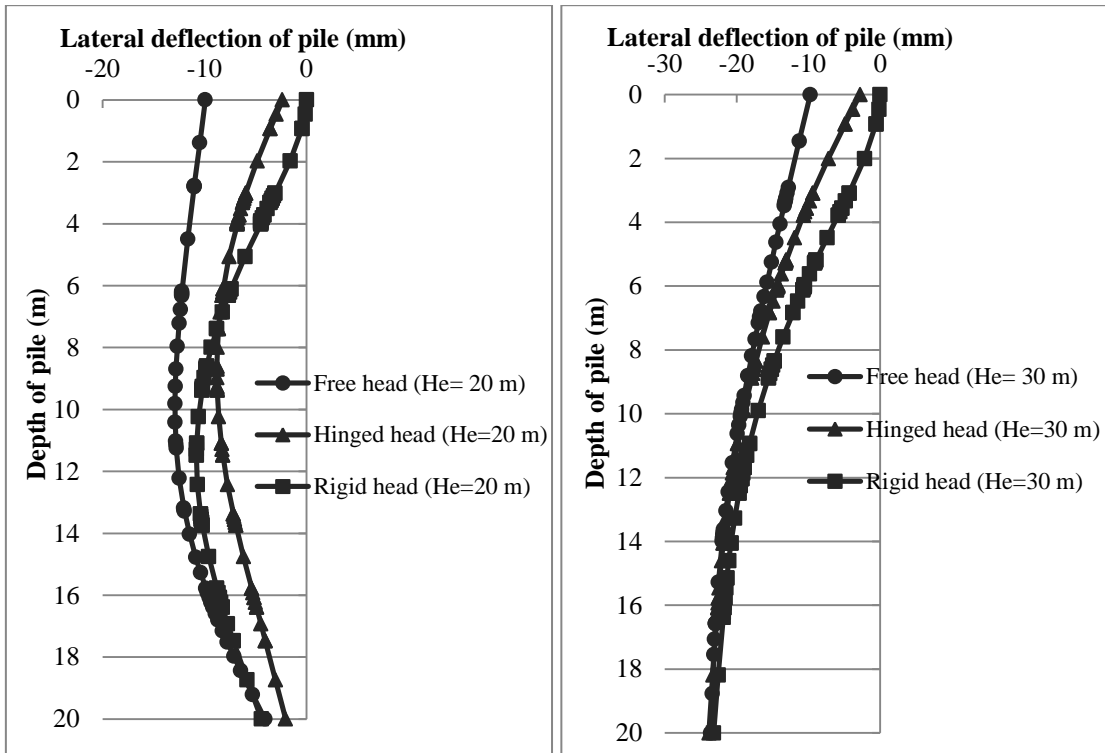
(b)   (c)

Figure 11:

The lateral deflection of pile in case of free, hinged and rigid pile head for case of (a) $H_e/L_p = 0.5$ (b) $H_e/L_p = 1$ (c) $H_e/L_p = 1.5$

(a)

(b)   (c)

Figure 12:

*The induced bending moment in case of free, hinged and rigid pile head for the case of **a.** $H_e/L_p = 0.5$ **b.** $H_e/L_p = 1$ **c.** $H_e/L_p = 1.5$*

CONFLICT OF INTEREST

Authors approves that to the best of his knowledge, there is not any conflict of interest or common interest with an institution/organization or a person that may affect the review process of the paper.

AUTHOR CONTRIBUTION

The authors together designed the study and wrote the paper. Sameh Ashour performed the literature, finite element analyses, interpretation and creating the manuscript. Yeşim S. Ünsever performed the determination of conceptual and/or design processes of the study, critical review of intellectual content, final approval and full liability of the study.

REFERENCES

1. ACI Committee 318. (2005) Buliding code requirements for structural concrete and commentary.

2. Bolton, M.D. and Powrie, W. (1986) The collapse of diaphragm walls retaining clay, *Geotechnique,* 37(3), 335-353. doi:10.1680/geot.1987.37.3.335

3. Choudhury, D., Shen, R.F., Leung, C.F. and Chow, Y.K. (2006) Centrifuge model study on pile responses due to adjacent excavation, *ASCE Geoshanghai International Conference, Shanghai,* 145–151. doi:10.1061/40865(197)18

4. Ding, W., Qiao, Y. 2014. Numerical Analysis of Pile Response to Deep Excavation in Soil Overlying Rock., *ASCE Geoshanghai 2014,* 700–709. doi: 10.1061/9780784413449.068

5. Goh, A.T.C., Wong, K.S., Teh, C.I., Wen, D. (2003) Pile response adjacent to braced excavation, *J. Geotech. and Geoenvrion. Eng., ASCE,* 129(4):383-396. doi:10.1061/(ASCE)1090-0241(2003)129:4(383)

6. Finno, R.J., Laurence, S.A., Allauh N.F., Harahap I.S. (1991) Analysis of performance of pile groups adjacent to deep excavation, *J. Geotech. Eng., ASCE,* 117(6), 934-55. doi:10.1061/(ASCE)0733-9410(1991)117:6(934)

7. Hsiung, B.C.B. (2009) A case study on the behaviour of a deep excavation in sand, *Computers and Geotechnics,* 36(4), 665-675. doi:10.1016/j.compgeo.2008.10.003

8. Leung, C.F., Chow, Y.K., Shen, R.F. (2000) Behavior of pile subject to excavation-induced soil movement, *J. Geotech. and Geoenvrion. Eng., ASCE,* 126(11), 947–954. doi: 10.1061/(ASCE)1090-0241(2000)126:11(947)

9. Leung, C.F., Lim, J.K., Shen, R.F., Chow, Y.K. (2003) Behaviour of pile Groups subject to excavation-induced soil movement, *J. Geotech. and Geoenvrion. Eng., ASCE,* 129(1), 58-65. doi:10.1061/(ASCE)1090-0241(2003)129:1(58)

10. Li, L., Hu, X., Dong, G., Liu, J. (2014) Three-Dimensional Numerical Analyses of Pile Response due to Braced Excavation-Induced Lateral Soil Movement, *Applied Mechanics and Materials,* 580-583:524-531. doi:10.4028/www.scientific.net/amm.580-583.524

11. Liyanapathirana, D.S., Nishanthan, R. (2016) Influence of deep excavation induced ground movements on adjacent piles, *Tunneling and Underground Space Technology,* 52, 168–181. doi:10.1016/j.tust.2015.11.019

12. Ng, C.W.W., Yau, T.L.Y., Li, J.H.M., Tang, W.H. (2001) New failure load criterion for large diameter bored piles in weathered geomaterials, *J. Geotech. and Geoenvrion. Eng., ASCE,* 127 (6), 488-498. doi:10.1061/(ASCE)1090-0241(2001)127:6(488)

13. Ng, C.W.W., Wei, J., Poulos, H. and Liu, H. (2017) Effects of multipropped excavation on an adjacent floating pile. *J. Geotech. and Geoenviron. Eng.,* ASCE, 143(7), 04017021. doi:10.1061/(ASCE)GT.1943-5606.0001696

14. Nishanthan, R., Liyanapathirana, D.S., Leo, C.J. (2016) Shielding effect in pile groups adjacent to deep unbraced and braced excavations. *Int. Journal of Geotech. Eng.,* 11(2):162-174. doi:10.1080/19386362.2016.1200270

15. Ong, D.E., Leung, C.F., Chow, K.Y. (2006) Pile behavior due to excavation-induced soil movement in clay. I: Stable Wall, *J. Geotech. Geoenviron. Eng.,* 132(1), 36-44. doi:10.1061/(ASCE)1090-0241(2006)132:1(36)

16. Poulos, H.G., Chen, L.T. (1996) Pile response due to unsupported excavation-induced lateral soil movement, *Canadian Geotech. Journal,* 33(4): 670-677. doi:10.1139/cgj-33-4-670

17. Poulos, H.G., Chen, L.T. (1997) Pile response due to excavation-induced lateral soil movement, *J. Geotech. and Geoenviron. Eng.,* ASCE, 123(2):94-99. doi:10.1061/(ASCE)1090-0241(1997)123:2(94)

18. PLAXIS Material Models CONNECT Edition V20.

19. Soomro, M.A., Mangnejo, D.A., Bhanbhro, R., Memom, N.A. (2019) 3D finite element analysis of pile responses to adjacent excavation in soft clay: Effects of different excavation depths systems relative to a floating pile, *J. Tunnelling and Underground Space Technology,* 86, 138-155. doi:10.1016/j.tust.2019.01.012

20. Shakeel, M. and Ng, C.W.W. (2017) Settlement and load transfer mechanism of pile group adjacent to a deep excavation in soft clay, *Comput. Geotech.,* 96, 55-72. doi:10.1016/j.compgeo.2017.10.010

21. Smulders, C.M., Hosseini, S., Brinkgreve, R.B.J. (2019) Improved embedded beam with interaction surface, *Proceedings of the XVII ECSMGE 2019*, Reykjavik, 1-8. doi:10.32075/17ECSMGE-2019-0139

22. Teh, K.L., Leung, C.F., Chow, Y.K. (2005) Spudcan penetration in sand overlying clay, *ISFOG 2005,* Perth, Australia, 529-534.

23. Ünsever, Y.S. (2015) An experimental study on static and dynamic behaviour of model pile foundations. PhD thesis, *ODTÜ Fen Bilimleri Enstitüsü, İnşaat Müh. Anabilim Dalı,* Ankara.

24. Yamashita, S., Jamiolkowski, M., Presti, D. C. L. (2000) Stiffness nonlinearity of three sands, *J. Geotech. Geoenviron. Eng., ASCE,* 126(10),929-942. doi:10.1061/(ASCE)1090-0241(2000)126:10(929)

25. Zhang, R., Zhang, W., Goh, A. (2018) Numerical investigation of pile responses caused by adjacent braced excavation in soft clays, *Int. J. Of Geotech. Engineering.,* 1-15. doi:10.1080/19386362.2018.1515810